# Photon-assisted Phase Slips in Superconducting Nanowires

Biao Zhang,[1] Labao Zhang[1,*] Qi Chen,[1] Yanqiu Guan,[1] Guanglong He,[1] Yue Fei,[1] Xiaohan Wang,[1] Jiayu Lyu,[1] Jingrou Tan,[1] Haochen Li,[1] Yue Dai,[1] Feiyan Li,[1] Hao Wang,[1] Shunli Yu,[2] Xuecou Tu,[1] Qingyuan Zhao,[1] Xiaoqing Jia,[1] Lin Kang,[1] Jian Chen,[1] and Peiheng Wu[1]

[1]*Research Institute of Superconductor Electronics, Nanjing University, Nanjing 210023, China*
[2]*School of Physics, Nanjing University, Nanjing 210023, China*

Phase slip is the intrinsic fluctuation of the order parameter and leads to the dissipation of superconductors. Here we propose a photon-assisted phase-slip model in superconducting nanowires to explain the phase-slip rate under photon irradiation. In this phenomenological model, incident photons destroy large quantities of Cooper pairs and reduce the free-energy barrier of phase slips, resulting in proliferation in the phase-slip events and leading to superconducting transition. The switching rates from the superconducting state of a niobium nitride nanowire under various photon irradiation (4.4 mW/m$^2$–4.4 W/m$^2$) and temperatures (2.3–3.7 K) are investigated through the distribution of switching currents in the experiment. The experimental data can be well fitted by our deduced expression of phase-slip rate after eliminating the influence of external noise. Our model develops the phase-slip theory under incident photons and is promising to reveal the intrinsic detection mechanism of the superconducting nanowire single-photon detector.

DOI: 10.1103/PhysRevApplied.17.014032

## I. INTRODUCTION

The superconducting nanowire single-photon detector (SNSPD) has been developed for 20 years after being proposed in 2001 [1]. It now has a system detection efficiency of more than 98% [2,3] and time jitter of fewer than 3 ps [4], and it has been applied in the photonic quantum computer [5], quantum communication [6], lidar [7,8], deep-space laser communication [9], and molecular fluorescence imaging [10]. Although the SNSPD has made significant progress in application, its photon-detection mechanism remains to be further studied [11].

The hotspot model proposed by Semenov *et al.* [12] predicts that the photon-induced hotspot is on the few nanometers to tens of nanometer scale. Therefore, one generally fabricates the SNSPD with the dimension of the width comparable to the size of a hotspot to achieve an infrared-sensitive single-photon detector. Besides, the diffusion-based vortex-entry model was proposed by Engel *et al.* in 2013 [13], which combines the generation and diffusion of quasiparticles after photon absorption with the formation of the normal-conducting cross section due to vortices. Later, the normal-core vortex model was developed by Zotova *et al.* [14], considering vortices entering from the edge and vortex-antivortex pairs being generated inside the superconducting strip. Recently,

the single-photon detection in micrometer-wide niobium nitride (NbN) bridges was experimentally achieved by Korneeva *et al.* in 2018 [15]. The authors demonstrated that the detection mechanism of the micrometer-wide NbN bridge is consistent with the improved theoretical modeling based on the theory of nonequilibrium superconductivity, including the vortex-assisted mechanism of initial dissipation. This is significant progress in single-photon detectors since the results prove that it is possible to detect single photons with microbridges and pave the way to the superconducting microwire single-photon detector. Nevertheless, the hotspot model suggests a long-wavelength cutoff in the quantum efficiency, while it has not been undoubtedly observed in experiments [16]. In addition, the vortex cannot exist in the nanowire with a width less than $4.4\xi$ demonstrated by Likharev *et al.* in 1979 [17], where $\xi$ is the superconducting coherence length, limiting the application of the vortex-crossing model in extremely narrow nanowires. Thus, the detection mechanism of the SNSPD remains to be studied, especially in the nanometer-wide superconductors.

Phase slip is the intrinsic fluctuation of superconductors, which is promising to develop a photon-detection mechanism of the SNSPD. Numerous experiments have been implemented to explore the phase-slip-based photon-detection mechanism of superconducting nanowires. In 2012, Delacour *et al.* [18] observed the thermal and quantum phase slip in the superconducting NbN nanowire

and investigated the photon detection with different wavelengths at various temperatures. It is found that phase slips are stable at the low temperature when no hot spot is formed, revealing the possibility of applying the phase-slip theory to explain the photon-detection mechanism of superconducting nanowires. Ejrnaes *et al.* [19] reported on measurements of the switching-current distributions on two-dimensional superconducting Nb-Ti-N strips at various temperatures from 0.3–4.0 K, and they observed that the width of the distributions has a nonmonotonous temperature dependence. They showed that the temperature dependence is caused by switching due to multiple fluctuations. Since the switching rate is reduced when it originates in multiple phase-slip events in the high-temperature region, these results could explain why SNSPDs based on Nb-Ti-N have lower dark-count rates. Kato *et al.* [20] studied the manipulation of the thermal and quantum phase slips in ultrathin niobium-nitride superconducting nanowires. They found that these nanowires exhibit resistive steps in current-voltage characteristics, and the nanowire length can tune the number of phase-slip centers (PSCs) in the nanowire. They also found that superconducting and PSC states can be switched by microwaves, and the emergence of each single PSC can be precisely controlled by varying the power of microwaves. In 2020, Lyatti *et al.* [21] observed strong evidence for energy-level quantization in the $YBa_2Cu_3O_{7-x}$ nanowire, and they showed that the absorption of a single photon could change the phase slip and quantum state of a nanowire, which was referred to as the phase-slip mechanism for photon detection. These works have not quantitatively analyzed how photons affect superconducting switching and fail to establish the mathematical relationship between photons and phase-slip rate. Further research is still required to reveal the phase-slip rate under photon irradiation.

Here we propose a photon-assisted phase-slip model in superconducting nanowires to explain the phase-slip rate under photon irradiation. In this phenomenological model, incident photons break down the superconductivity of the nanowire and reduce the free-energy barrier of phase slips, resulting in a dramatic increase in the phase-slip rate and triggering the photon response. A single phase-slip event in the low-temperature region releases enough heat to induce a switching event in the nanowire [22,23], as in an underdamped Josephson junction [24]. In the high-temperature region, multiple phase slips dominate, and multiple phase slips trigger a superconducting transition event [22,23]. When photons are incident, the phase-slip events increase, increasing the superconducting transition events regardless of the low- or high-temperature region, thus increasing the photon response. We quantitatively investigate the relationship between incident photons and phase-slip rate by measuring the distribution of superconducting switching current $I_{sw}$ under photon irradiation. We find that the phase-slip rate increases with temperature and laser

irradiance $I_{laser}$. We propose the reduction of free-energy barrier $F(E, T)$ caused by photon irradiation and establish the quantitative relationship between the phase-slip rate $\Gamma_{PS}(I, T, E)$ and $F(E, T)$. Our model develops the phase-slip theory under incident photons. The parameters $k_T$ and $k_p$ in our model denote the reduction of free-energy barrier caused by the temperature rise and incident photons, respectively. We show that the model agrees well with the experimental data, and our findings are promising to develop into a photon-detection mechanism of the SNSPD and instruct the design of high-performance devices.

## II. SAMPLE AND CHARACTERIZATION

We fabricate an 80-$\mu$m-long NbN nanowire and measure the *R-T* and *I-V* curves of the nanowire. First, the NbN film with a thickness of 6 nm is deposited by magnetron sputtering on a $Si_3N_4$ substrate, and then the gold electrode is fabricated by photolithography and liftoff. Finally, the 80-nm-wide NbN nanowire is fabricated using electron-beam lithography and reactive ion etching. The detailed description of our method can be found in Appendix A and our previous works [25,26]. The critical current $I_c$ of the nanowire is measured to be 13 $\mu$A at the temperature of 2.3 K, and the *R-T* curves at various bias currents $I_b$ are measured, as shown in Fig. 1(a). From right to left, $I_b$ gradually increases from $0.02I_c$ to $0.87I_c$. After $I_b > 0.35I_c$, the *R-T* curve shows a three-stage superconducting transition. The two transitions in higher temperature are transitions of NbN electrodes with broader width, and the transition in the lowest temperature is of the narrowest NbN nanowire [22]. After $I_b > 0.87I_c$, the nanowire enters a latching state and no longer exhibits a superconducting transition. Different curves show the same local transition at certain temperatures, such as 3.5 K, indicating a phase-slip center in the nanowire [18]. The low-pass filter is used to suppress the noise of the circuit, and the measurement environment is well electromagnetically shielded. The detailed measurement system can be found in Appendix A.

The nanowire undergoes two sorts of phase slips when the temperature is lower than $T_c$, i.e., the thermally activated phase slip (TAPS) [27] and quantum phase slip (QPS) [28,29]. TAPS affects the superconducting transition in the immediate vicinity of $T_c$ and QPS occurs at any temperature lower than $T_c$. QPS can thoroughly wash out the superconducting order even as temperature approaches 0 K, resulting in the so-called superconducting-insulation transition (SIT). The *R-T* curve of the nanowire affected by the two phase slips can be described by corresponding theoretical models. In order to confirm the phase slips of the nanowire, we select the *R-T* curve at $0.02I_c$ for further analysis. We use Little's model [18,27] to estimate the
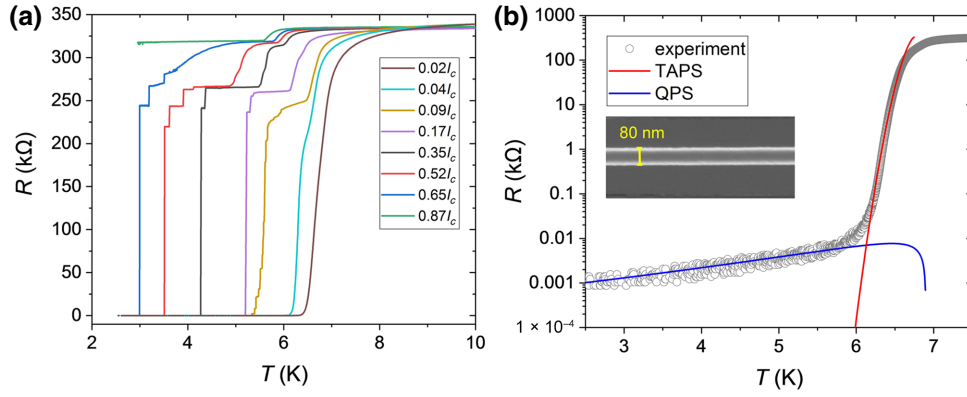
FIG. 1. Resistance-temperature curves for the 80-nm-wide NbN nanowire. (a) $R$-$T$ curves under increasing bias currents from $0.02I_c$ to $0.87I_c$ from right to left. $I_c$ is measured to be 13 $\mu$A at the temperature of 2.3 K. (b) Fits of the $R$-$T$ curve at a low current bias (2% of $I_c$) using thermal (red line) and quantum (blue line) phase-slip models. The circles are the data, and the fitting equations are Eqs. (1) and (2) in the text, respectively. Inset: scanning electron micrograph of part of the nanowire. The wider NbN electrodes are not shown in the figure.

contribution of TAPS:

$$R_{\text{TAPS}}(T) = R_n \exp\left(-\frac{\Delta F(T)}{k_B T}\right), \qquad (1)$$

where $\Delta F(T) = 0.83 k_B T_c R_q wd(1 - T/T_c)^{3/2}/[\rho\xi(0)]$ is the temperature-dependent superconducting condensation energy, $k_B$ is the Boltzmann constant, $R_q = h/4e^2 \sim 6.5$ k$\Omega$ is the quantum resistance, $w$ and $d$ are the width and thickness of the nanowire, $\rho = 1.97$ $\mu\Omega$ m is the resistivity of the nanowire, $\xi(0) = 6$ nm is the coherence length in the 0 K limit [18] and $R_n = 328$ k$\Omega$ is the normal resistance of the nanowire. We obtain an excellent fitting result using these parameters when $T \sim T_c$, shown by the red line in Fig. 1(b).

When the temperature is much lower than $T_c$, the quantum phase slip caused by the quantum fluctuation of the order parameter dominates, and the resistance given by Little's model drops rapidly. We use the theory proposed by Golubev *et al.* [28,29] to fit the resistance caused by QPS:

$$R_{\text{QPS}}(T) = BR_q S_{\text{QPS}} \frac{L}{\xi(T)} exp(-S_{\text{QPS}}), \qquad (2)$$

where $S_{\text{QPS}} = CR_q L/[R_n\xi(T)]$ is the effective action. The QPS rate is determined by $S_{\text{QPS}}$, and the dissipation of quasiparticles and the electromagnetic wave propagating along the nanowire when QPS occurs are both considered. $L = 80$ $\mu$m is the length of the nanowire, $\xi(T) = \xi(0)(1 - T/T_c)^{-1/2}$ is the temperature-dependent coherence length, $R_n$ and $\xi(0)$ are the same as those used in TAPS fitting, $B$ and $C$ are fitting factors. We obtain $B = 1.3 \times 10^{-6}$ and $C = 0.03$ after several iterations, and the fitting result is shown in Fig. 1(b) in the blue line. The fit provides an accurate agreement with the resistive tail of the nanowire in the measured temperatures, showing a crossover between TAPS and QPS regimes.

We measure the $I$-$V$ curves of the nanowire at the temperature ranges from 2.3 to 4.3 K, and the current sweep rate is 0.67 $\mu$A/s. A representative set of $I$-$V$ curves is shown in Fig. 2(a). The current at which the switching occurs is called switching current $I_{\text{sw}}$, and as the bias current is swept from high to low, the nanowire reverts to being superconducting at the retrapping current $I_r$. It can be seen that $I_{\text{sw}}$ varies significantly at different temperatures, while $I_r$ is almost the same, indicating that the thermal relaxation efficiency between the nanowire and the substrate keeps constant among the measured temperatures.

We perform 2000 $I$-$V$ sweeps at each temperature to measure $I_{\text{sw}}$ fluctuations. For each distribution, we calculate the mean value $\langle I_{\text{sw}}\rangle$ and the standard deviation $\delta I_{\text{sw}}$ as shown in Fig. 2(b). As the temperature rises, $\langle I_{\text{sw}}\rangle$ and $\delta I_{\text{sw}}$ gradually decrease. We use the phenomenological equation $I_c = I_{c0}[1 - (T/T_c)^2]^{3/2}$ to fit $\langle I_{\text{sw}}\rangle$ [30] and get a good agreement shown in the blue line. As the temperature increases, the number of Cooper pairs decreases, thus $\langle I_{\text{sw}}\rangle$ decreases accordingly. In the relatively high-temperature regime, more phase slips are required to trigger the superconducting transition, so the switching tends to occur in a very narrow range close to $I_c$, thus $\delta I_{\text{sw}}$ decrease in the high temperature [22].

## III. PHASE SLIPS UNDER PHOTON IRRADIATION

We irradiate the nanowire with a continuous near-infrared laser to investigate the relationship between incident photons and phase-slip rate. The wavelength and $I_{\text{laser}}$ are 1310 nm and 4.4 mW/m², respectively, and the temperature is increased from 2.3 to 3.7 K. We perform 2000 $I$-$V$ sweeps at each temperature. The distribution of $I_{\text{sw}}$ is shown in Fig. 3(a). The overall trend of $I_{\text{sw}}$ with temperature does not change under light irradiation, and both $\langle I_{\text{sw}}\rangle$
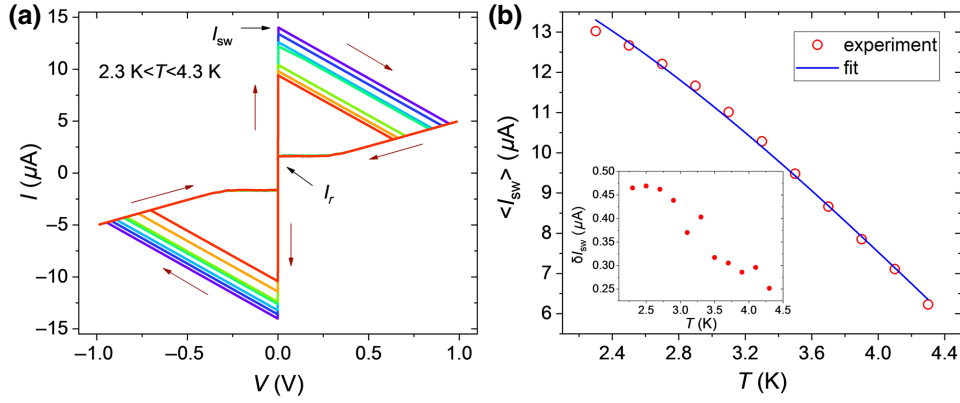
FIG. 2. Current-voltage characterization without light irradiation. (a) *I-V* curves at temperature ranging from 2.3 to 4.3 K. The switching current $I_{sw}$ and retrapping current $I_r$ are indicated at 2.3 K. (b) Red circle: the mean value of $I_{sw}$ ($\langle I_{sw} \rangle$) from 2.3 to 4.3 K. Blue line: fitting result using the theory proposed by Bardeen. Inset: the standard deviation of $I_{sw}$ ($\delta I_{sw}$) from 2.3 to 4.3 K.

and $\delta I_{sw}$ decrease with the increase of temperature. The $I_{sw}$ distributions at various temperatures reflect the collective dynamics of random fluctuations of the order parameter and provide a powerful tool for revealing the essence of quasi-one-dimensional superconductivity. This method was proposed by Fulton *et al.* [24] in 1974 when they studied the Josephson junction. The relationship between the distribution of $I_{sw}$ and the switching rate $\Gamma_{sw}(I)$ is as follows:

$$P(I) = \Gamma_{sw}(I)\left(\frac{dI}{dt}\right)^{-1}\left(1 - \int_0^I P(u)du\right), \quad (3)$$

where $P(I)$ is the distribution of $I_{sw}$, $\Gamma_{sw}(I)$ is the superconducting switching rate at current $I$, $dI/dt$ is the current sweep rate, and one can extract $\Gamma_{sw}(I)$ from $P(I)$ based on Eq. (3), in principle. Although there is no analytical solution for $\Gamma_{sw}(I)$, we get the numerical solution utilizing the method proposed by Fulton *et al.*, and the results are shown by the circles in Fig. 3(c). Similarly, $P(I)$ is measured as the $I_{laser}$ gradually increased from 4.4 mW/m² to 4.4 W/m² at the fixed temperature of 2.7 K, and the corresponding optical attenuation is from −30 to 0 dB. The results are shown in Fig. 3(b). We utilize the same method to extract $\Gamma_{sw}(I)$ from $P(I)$ under various $I_{laser}$, and the results are shown as the circles in Fig. 3(d).

The energy released by each phase slip is $hI/2e$, $h$ is Planck's constant, and $e$ is the elementary charge. For the 10 $\mu$A current used in the experiment, the energy released by each phase slip is approximately 0.13 eV, and the energy of a single photon with the 1310-nm wavelength is approximately 0.94 eV, which is approximately 7.23 times the energy released by a single phase slip. Thus, the single-photon incidence is sufficient to trigger enough phase slips from the perspective of energy. In the absence of incident photons, the TAPS rate $\Gamma_{PS}(I, T) = \Omega(T)\exp[-\Delta F(I, T)/k_B T]$, where

$\Omega(T) = L/(\xi(T)\tau_{GL})(\Delta F(I, T)/k_B T)^{1/2}$ is the attempt frequency, $\tau_{GL} = \pi\hbar/[8k_B(T_c - T)]$ is the Ginzburg-Landau time, and $\Delta F(I, T) = (2.45\hbar/2e)I_c(T)[1 - I/I_c(T)]^{3/2}$ is the free-energy barrier [23]. Incident photons destroy a large number of Cooper pairs, leading to a sharp increase in phase slips, which is equivalent to reducing the free-energy barrier $\Delta F(I, T)$. Considering both the TAPS and QPS rate of the nanowire, we propose the following equation to describe the phase-slip rate $\Gamma_{PS}(I, T, E)$ under photon irradiation:

$$\Gamma_{PS}(I, T, E) = \Omega(T)\exp\left(-\frac{F(I, T) - F(E, T)}{k_B(T + T_{QPS})}\right), \quad (4)$$

where $F(E, T)$ denotes the reduction of the free-energy barrier at temperature $T$ when photons irradiate the nanowire with total energy $E$. $T_{QPS}$ is the "quantum" temperature caused by QPS, which is a common and well-tested approach in Josephson junctions [31] and superconducting nanowires [22]. $T_{QPS} = \hbar/2\pi k_B(LC)^{0.5}$ represents the strength of zero-point fluctuations in the *LC* circuit formed by the nanowire. In our experiment, the nanowire has a nonzero kinetic inductance of approximate 1 nH and a mutual capacitance of the order of approximate 5 fF of the leads. Thus, we can estimate the plasma frequency as $1/(LC)^{0.5}$, and we get the expected quantum temperature $T_{QPS} \sim 1$ K.

As temperature rises, the energy gap of the superconductor decreases, and the phase-slip rate increases. Thus, $F(E, T)$ is positively correlated with $T$. Similarly, as total incident energy $E$ increases, the Cooper pairs broken by incident photons increase, resulting in the further suppressed superconductivity and increasing phase-slip rate. $F(E, T)$ shows a positive correlation with $\ln(E/h\nu)$ using the logarithmic form of the incident photons' number. The temperature range of the experiment is 2.3–3.7 K, which is relatively limited and in the same order of magnitude.
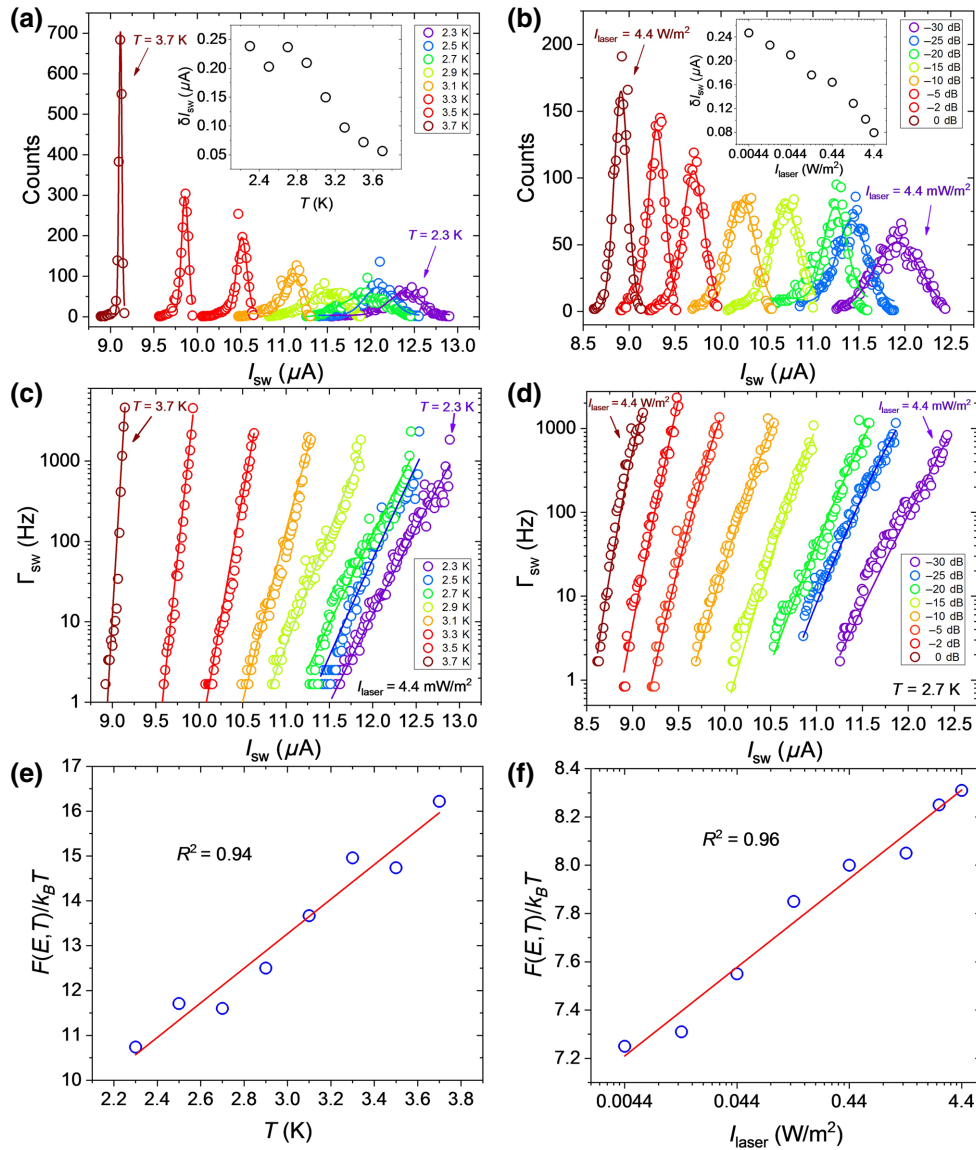
FIG. 3.   Switching current measurements and theoretical fitting results at different temperatures and laser irradiation. (a) The distribution of $I_{sw}$ at various temperatures. The laser irradiation $I_{laser}$ is fixed at 4.4 mW/m$^2$, and the temperature is increased from 2.3 to 3.7 K. Inset: the $\delta I_{sw}$ at various temperatures. (b) The distribution of $I_{sw}$ at various $I_{laser}$. The temperature is fixed at 2.7 K and $I_{laser}$ is increased from 4.4 mW/m$^2$ to 4.4 W/m$^2$, with corresponding light attenuation from $-30$ to 0 dB. Inset: the $\delta I_{sw}$ at various $I_{laser}$. (c) Circles: the distribution of superconducting switching rate $\Gamma_{sw}$ obtained from (a). Solid lines: fitting results utilizing the photon-assisted phase-slip model. (d) Circles: the distribution of $\Gamma_{sw}$ obtained from (b). Solid lines: fitting results utilizing the photon-assisted phase-slip model. (e) Blue circles: the relationship between $F(E, T)/k_B T$ and $T$ extracted from the fitting results of (c). Red line: linear fit of $F(E, T)/k_B T$ and $T$. (f) Blue circles: the relationship between $F(E, T)/k_B T$ and $E$ (logarithmic coordinate) extracted from the fitting results of (d). Red line: linear fit of $F(E, T)/k_B T$ and $E$.

Thus the linear relationship with temperature is an appropriate model for the experiment. The range of incident photon energy $E$ is relatively large, and the dynamic range of incident energy is 30 dB. Thus, the logarithmic relationship is conducive to simplifying the model and analysis. Moreover, we think that this logarithmic form is related to the change of entropy due to Cooper-pair breaking caused by photons, which leads to a variation of the free energy.

The value of $E/h\nu$ is the number of photons and thus corresponds to the number of Bogoliubov quasiparticles induced by the photons. The entropy is logarithmically dependent on the number of quasiparticles, so the free-energy variation caused by incident photons should have the form of $\ln(E/h\nu)$. The energy of incident photons passes through the electron-phonon system and finally transfers to the substrate for dissipation. The duration of

the whole process is generally tens of picoseconds [23,32]. Therefore, the nanowire temperature does not increase significantly due to the photon incidence before phase slips occur. Thus $E$ and $T$ are two independent variables for $F(E, T)$. In summary, we get the expression of $F(E, T)$ as

$$F(E, T) = \left( k_T T + k_p \ln \frac{E}{h\nu} + k_0 \right) k_B T. \qquad (5)$$

In Eq. (5), $k_T$ is the temperature coefficient with the unit of $K^{-1}$, denoting the relative value of the reduction of the free-energy barrier for each 1-K temperature rise. The superconductor with strong electron-phonon coupling and the phonon-phonon coupling has a higher $k_T$, and such superconductors generally have high thermal conductivity. $k_p$ is a dimensionless coefficient, which represents the free-energy barrier reduction caused by incident photons. $k_p$ demonstrates the suppression of the free-energy barrier by incident photons, and the more Cooper pairs destroyed by an incident photon, the higher $k_p$ is, which implies that the superconductor with a lower energy gap has a higher $k_p$. $k_0$ is a dimensionless correction constant considering the energy loss caused by the radiation of electromagnetic waves when a phase slip occurs. The phase-slip rate is more profound in nanowires with small cross sections, which implies that narrow nanowires have a higher $k_0$. We use Eqs. (4) and (5) to fit the data in Figs. 3(c) and 3(d), and the solid lines show the results. It can be seen that the superconducting switching of the nanowire under different photon irradiation and temperatures is consistent with Eq. (4), which in turn verify the photon-assisted phase-slip model.

In order to verify the linearity of Eq. (5), we plot the relationship between $F(E, T)/k_B T$ and $T$ and $E$ (logarithmic coordinate), as shown in Figs. 3(e) and 3(f). The coefficient of determination ($R^2$) of linear fitting results is 0.94 and 0.96, respectively, indicating that $F(E, T)$ has a good linear relationship with $T$ and $\ln E$. We get $k_T = 3.87 \pm 0.71$ $K^{-1}$, $k_p = 0.15 \pm 0.03$, and $k_0 = 6.60 \pm 2.23$ from the linear fitting results, with the confidence bound of 95%. Equations (4) and (5) fit the 16 sets of data in Fig. 3 consistently, showing a certain universality of the model under the experiment environment. The model indicates that the phase-slip rate under illumination increases with $k_T$ and $k_p$, which increases the photon-response probability. Superconductors with low energy gap and high thermal conductivity have higher $k_p$ and $k_T$, which are conducive to developing the SNSPD with high detection efficiency. However, we need to point out that this model is applicable to narrow wires and might not work in microwires. Phase slips mainly occur in one-dimensional superconductors, i.e., the superconductors with thickness and width in the same order of the coherence length, while the width of

the microwire far exceeds the coherence length. The free-energy barrier of phase slip is proportional to the cross-section area of the nanowire [33], which will increase with the cross-section area of the microwire, and the phase-slip rate will decrease significantly.

$\langle I_{sw} \rangle$ and $\delta I_{sw}$ under various laser irradiance and temperatures are studied to confirm that the distribution of $I_{sw}$ is caused by incident photons rather than external noise. $I_{laser}$ is increased from 4.4 to 139.1 mW/m$^2$ with the corresponding optical attenuation reduced from $-30$ to $-15$ dB, and the temperature is increased from 2.3 to 4.3 K. We perform 2000 $I$-$V$ sweeps at each temperature and photon irradiation, and results are shown in Fig. 4 and Appendix B. $\langle I_{sw} \rangle$ monotonically decreases as the temperature and $I_{laser}$ increases. $\delta I_{sw}$ shows a decreasing trend as the temperature increases, while it has no apparent dependence on $I_{laser}$. We measure the distribution of $I_r$ under different $I_{laser}$, and get the mean value of 1.68 $\mu$A and the standard deviation of 4.06 nA. The mean value and standard deviation of $I_r$ have no apparent dependence on the $I_{laser}$, indicating that the decrease of $I_{sw}$ is not caused by external noise but mainly caused by the intrinsic dynamics of the nanowire induced by the incident photons [21]. The dependence of $\langle I_{sw} \rangle$ on temperature predicted by BCS theory is no longer applicable because incident photons destroy large quantities of Cooper pairs. We propose the equation $I_c = I_{c0}\{1 - [(T - T_0)/T_c]^2\}^k$ and get a good fitting result, as shown by the solid lines in the upper part of Fig. 4. $T_0 = 2.1$ K is obtained from the fitting result, indicating that the $I_{sw}$ approaches saturation when the temperature is lower than 2.1 K, which means that the incident photons make the combination of Cooper pairs have a
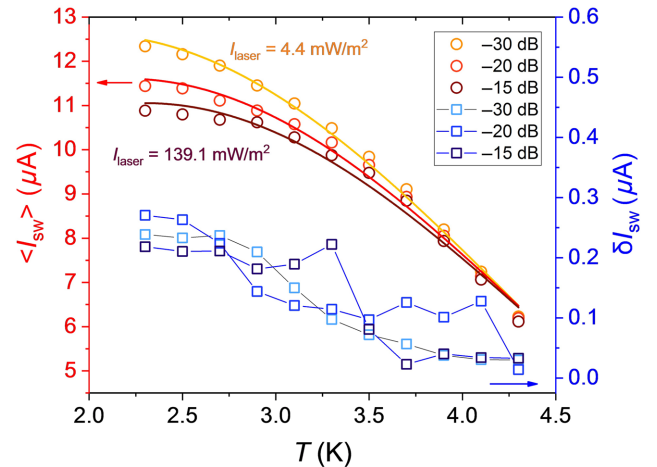


FIG. 4. The $\langle I_{sw} \rangle$ and $\delta I_{sw}$ under various $I_{laser}$ and temperatures. The $I_{laser}$ is increased from 4.4 to 139.1 mW/m$^2$, and the corresponding optical attenuation is $-30$, $-20$, and $-15$ dB, respectively. The circles are $\langle I_{sw} \rangle$, and the square boxes are $\delta I_{sw}$. The solid lines in the upper part are fitting results, and the lines in the low part are provided to guide the eye.
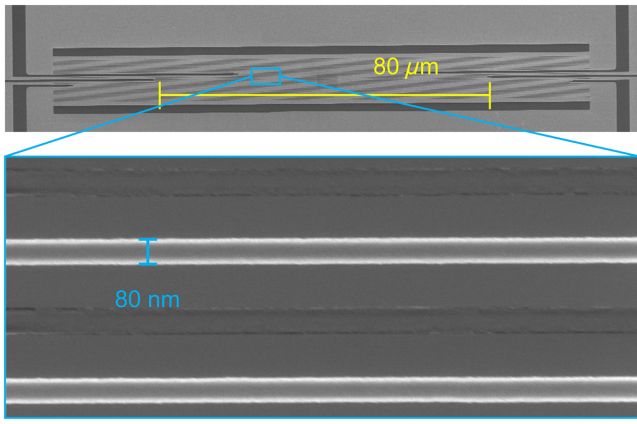
FIG. 5. Scanning electron micrograph of the nanowire. The length and the width of the NbN nanowire are 80 $\mu$m and 80 nm, respectively.

cutoff temperature higher than 0 K. $k$ denotes the compression index of $I_{sw}$ by incident photons, which represent the ability of the unbinding of Cooper pairs. $k = 2$ when no photons are incident [30], and $k$ is 2.9–3.8 in this experiment. $k$ increases with $I_{laser}$, and the unbinding effect on Cooper pairs of incident photons increases with $I_{laser}$ as well. The above results indicate that the incident photons hinder the combination of the Cooper pairs, leading to an increase in the phase-slip rate, confirming the reliability of the photon-assisted phase-slip model.

Currently, several theories have been proposed to explain the detection mechanism of SNSPD, for instance, the diffusion-based hotspot model [16], diffusion-based vortex-entry model [13,34], photon-triggered vortex-entry model [35], and the normal-core vortex model [36,37]. These theories study the dynamics of the hotspot, vortex, and quasiparticles. They establish the relationship between the threshold current $I_{th}$ and the photon energy $E$, but they all have limitations. The diffusion-based hotspot model predicts a thresholdlike response: the detector responds to all photons of a particular energy, or it does not, which

is not observed in the experiment [32]. The diffusion-based vortex-entry model cannot explain the temperature dependence of zero-energy extrapolated threshold current $I_0$ deduced from quantum-detector tomography (QDT) [11]. Until now, no theory can simultaneously explain the photon-detection dependence on the temperature, magnetic field, and the hit position on the nanowire. Our model focuses on phase slips and reveals the relationship between incident photons and superconducting switching through the influence of the energy barrier. The superconducting wave function elucidates the spatial distribution of all superconducting electrons, and phase slips reflect the statistical behavior of a large number of superconducting electrons. Thus, our theory studies the detection mechanism of the SNSPD from a relatively macroscopic perspective, and it is possible to develop a detection model that can avoid the problems encountered by the previous theories. In addition, QDT experiments have proven that the detector response is determined only by the total absorbed energy irrespective of the photons' number [32], which is also consistent with our model. Besides, the thermally activated and quantum phase slips have been suggested to explain the origin of the dark counts [38,39], and our model provides a possibility to unify the explanation of dark counts and photon response.

## IV. CONCLUSIONS

We propose a photon-assisted phase-slip model and establish the mathematical relationship between incident photons and phase-slip rate. In this phenomenological model, incident photons destroy a large number of Cooper pairs and reduce the free-energy barrier of the phase slip, resulting in a sharp increase in the phase-slip rate. We fabricate a superconducting NbN nanowire and investigate the superconducting switching of the nanowire under different laser irradiance and temperatures. Experimental data can be well explained by the model, confirming the reliability of the photon-assisted phase-slip model. This model develops the phase-slip theory under incident photons, and
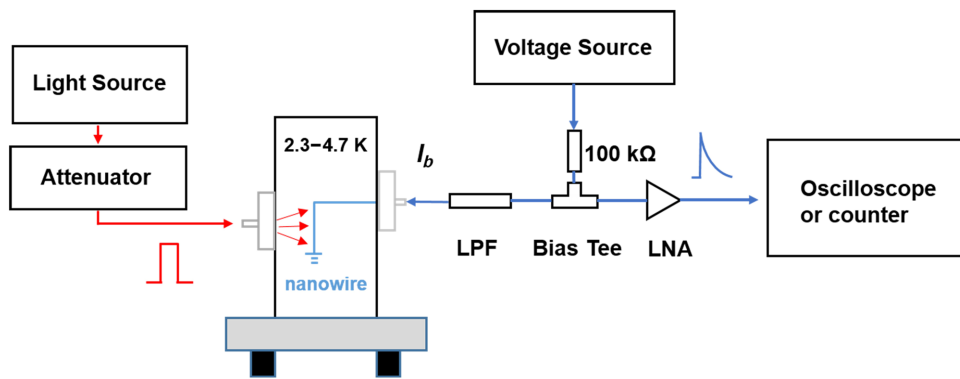


FIG. 6. Schematic diagram of the nanowire characterization.

it is promising to instruct the design of high-performance devices and develop into a detection model of the SNSPD.

## APPENDIX A: DEVICE FABRICATION AND CHARACTERIZATION

First, a thin film of NbN with a thickness of 6 nm is deposited on the $Si_3N_4$ substrate by dc magnetron sputtering. Then, an Au electrode with a thickness of approximately 200 nm is fabricated by photolithography. After the liftoff process, the Au electrode is prepared, and electron-beam exposure is initiated. The NbN film is spin coated with electron-beam photoresist (Hydrogen Silsesquioxane Polymers, HSQ) and is then baked for 4 min on a baking table at a temperature of 90 °C. After baking, the electron-beam exposure is started when the substrate temperature decreases to room temperature. During the process of electron-beam exposure, the current of the electron beam is set to 0.2 nA, the acceleration voltage is set to 100 kV, and the exposure is set to 1400 $\mu C/cm^2$. The nanowire pattern is generated by the exposure of the electron-beam lithography system, and the development runs at room temperature. Finally, the NbN nanowire is obtained by etching with a reactive ion-etching tool. The SEM image of the nanowire is presented in Fig. 5.

Figure 6 shows the electrical and optical system of the nanowire characterization. The nanowire is installed in a Gifford-McMahon refrigerator, and the temperature can be precisely adjusted. The laser passes through the adjustable attenuator, and then it is coupled to the nanowire by an optical fiber. The bias current ($I_b$) passes through a 100-k$\Omega$ resistor and then couples to the nanowire through a bias tee and a low-pass filter (LPF). The LPF is used to suppress the high-frequency noise from the voltage source. The voltage source has the measurement function and can be used to analyze the dc characteristics of the nanowire. The pulse from the nanowire passes through the rf end of the bias tee, and then it is input to an oscilloscope or counter through a low-noise amplifier (LNA) for further analysis.
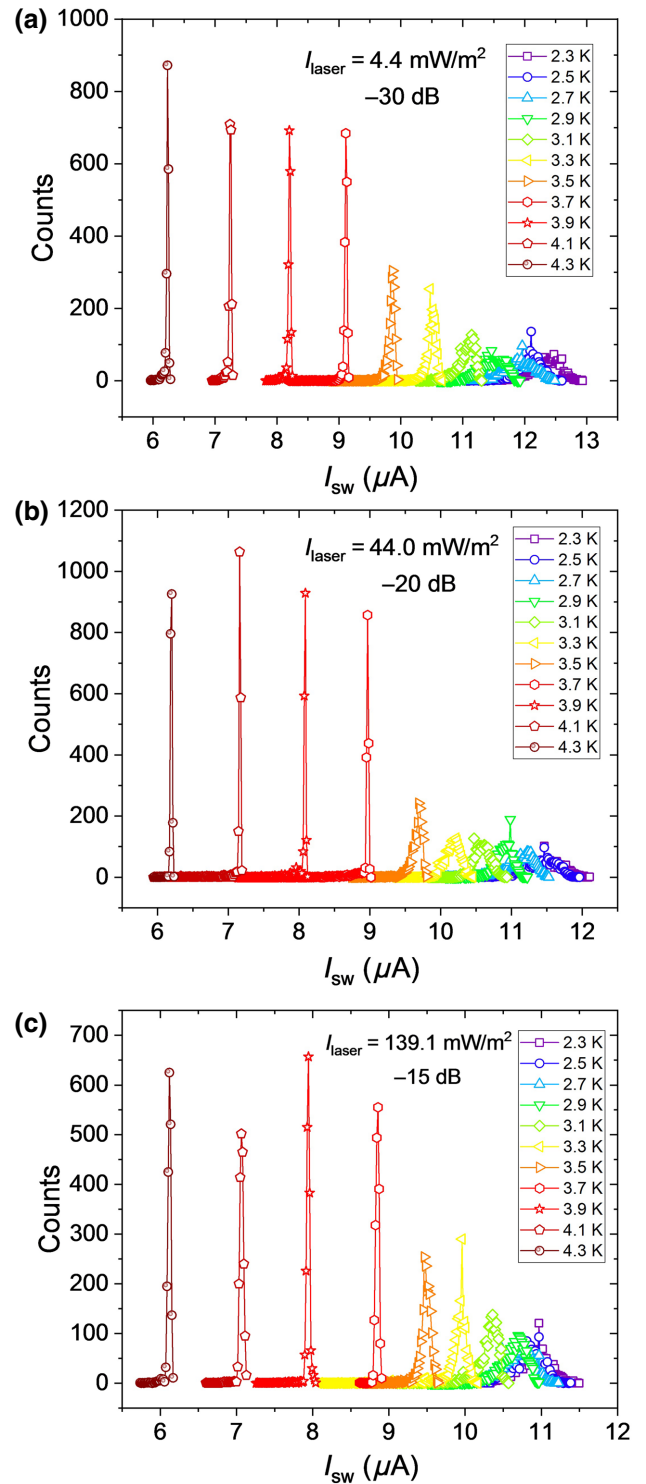


FIG. 7. The temperature dependence of $I_{sw}$ for different light irradiation. $I_{laser}$ is increased from 4.4 to 139.1 mW/m$^2$ and the temperature is increased from 2.3 to 4.3 K.

The typical *I-V* curve of superconducting nanowires is a strong hysteresis curve, as shown in Fig. 2(a). The current-voltage characteristic is measured using a voltage source

and a 100-kΩ resistor, as shown in Fig. 6. As the voltage increases, the nanowire exhibits an abrupt transition from an extremely low-voltage state ($<10$ mV) to a high-voltage state ($>100$ mV), i.e., from the superconducting state to the normal state. The maximum bias current that maintains the nanowire in the superconducting state is taken as the switching current $I_{sw}$, also known as the critical current $I_c$ in the bibliography. We measure the critical current $I_c$ several times at a fixed temperature, then take the average value $I_{c,ave}$, and we get $J_c$ using $I_{c,ave}$ divided by the cross-section area. The width of the nanowire is measured using the scanning electron microscope, and the thickness is calculated based on the dc magnetron sputtering rate and sputtering time. The measuring circuit does not use the shunt resistor.

## APPENDIX B: SUPPLEMENTARY EXPERIMENTAL DATA

The temperature dependence of $I_{sw}$ for different light irradiation is shown in Fig. 7. $I_{laser}$ is increased from 4.4 to 139.1 mW/m$^2$ with the corresponding optical attenuation reduced from $-30$ to $-15$ dB, and the temperature is increased from 2.3 to 4.3 K. We perform 2000 $I$-$V$ sweeps at each temperature and photon irradiation.

---

[1] G. N. Gol'tsman, O. Okunev, G. Chulkova, A. Lipatov, A. Semenov, K. Smirnov, B. Voronov, A. Dzardanov, C. Williams, and R. Sobolewski, Picosecond superconducting single-photon optical detector, Appl. Phys. Lett. **79,** 705 (2001).

[2] J. Chang, J. W. N. Los, J. O. Tenorio-Pearl, N. Noordzij, R. Gourgues, A. Guardiani, J. R. Zichi, S. F. Pereira, H. P. Urbach, V. Zwiller, S. N. Dorenbos, and I. Esmaeil Zedeh, Detecting telecom single photons with $(99.5 + 0.5–2.07)\%$ system detection efficiency and high time resolution, APL Photonics **6,** 036114 (2021).

[3] V. Reddy D, R. R. Nerem, S. W. Nam, R. P. Mirin, and V. B. Verma, Superconducting nanowire single-photon detectors with 98% system detection efficiency at 1550 nm, Optica **7,** 1649 (2020).

[4] B. Korzh, *et al.*, Demonstration of sub-3 ps temporal resolution with a superconducting nanowire single-photon detector, Nat. Photonics **14,** 250 (2020).

[5] H. S. Zhong, *et al.*, Quantum computational advantage using photons, Science **370,** 1460 (2020).

[6] Z. Wang, S. Miki, and M. Fujiwara, Superconducting nanowire single-photon detectors for quantum information and communications, IEEE J. Sel. Top. Quant. **15,** 1741 (2009).

[7] B. Zhang, Y. Q. Guan, L. H. Xia, D. X. Dong, Q. Chen, C. Xu, C. Wu, H. X. Huang, L. B. Zhang, L. Kang, J. Chen, and P. H. Wu, An all-day lidar for detecting soft targets over 100 km based on superconducting nanowire single-photon detectors, Supercond. Sci. Technol. **34,** 034005 (2021).

[8] L. Xue, Z. L. Li, L. B. Zhang, D. S. Zhai, Y. Q. Li, S. Zhang, M. Li, L. Kang, J. Chen, P. H. Wu, and Y. H. Xiong, Satellite laser ranging using superconducting nanowire single-photon detectors at 1064 nm wavelength, Opt. Lett. **41,** 3848 (2016).

[9] M. E. Grein, A. J. Kerman, E. A. Dauler, M. M. Willis, B. Romkey, R. J. Molnar, B. S. Robinson, D. V. Murphy, and D. M. Boroson, in *Conference on Advanced Photon Counting Techniques IX* (2015).

[10] J. Yu, R. L. Zhang, Y. F. Gao, Z. H. Sheng, M. Gu, Q. C. Sun, J. L. Liao, T. Wu, Z. Y. Lin, P. H. Wu, L. Kang, H. Li, L. B. Zhang, and W. Zheng, Intravital confocal fluorescence lifetime imaging microscopy in the second near-infrared window, Opt. Lett. **45,** 394684 (2020).

[11] J. J. Renema, R. Gaudio, Q. Wang, Z. Zhou, A. Gaggero, F. Mattioli, R. Leoni, D. Sahin, M. J. A. de Dood, A. Fiore, and M. P. van Exter, Experimental Test of Theories of the Detection Mechanism in a Nanowire Superconducting Single Photon Detector, Phys. Rev. Lett. **112,** 117604 (2014).

[12] A. D. Semenov, G. N. Gol'tsman, and A. A. Korneev, Quantum detection by current carrying superconducting film, Phys. C **351,** 349 (2001).

[13] A. Engel and A. Schilling, Numerical analysis of detection-mechanism models of superconducting nanowire single-photon detector, J. Appl. Phys. **114,** 214501 (2013).

[14] A. N. Zotova and D. Y. Vodolazov, Photon detection by current-carrying superconducting film: A time-dependent ginzburg-landau approach, Phys. Rev. B **85,** 024509 (2012).

[15] Y. P. Korneeva, D. Y. Vodolazov, A. V. Semenov, I. N. Florya, N. Simonov, E. Baeva, A. A. Korneev, G. N. Goltsman, and T. M. Klapwijk, Optical Single-Photon Detection in Micrometer-Scale NbN Bridges, Phys. Rev. Appl. **9,** 064037 (2018).

[16] A. Semenov, A. Engel, H. W. Hubers, K. Il'in, and M. Siegel, Spectral cut-off in the efficiency of the resistive state formation caused by absorption of a single-photon in current-carrying superconducting nano-strips, Eur. Phys. J. B **47,** 495 (2005).

[17] K. K. Likharev, Superconducting weak links, Rev. Mod. Phys. **51,** 101 (1979).

[18] C. Delacour, B. Pannetier, J. C. Villegier, and V. Bouchiat, Quantum and thermal phase slips in superconducting niobium nitride (NbN) ultrathin crystalline nanowire: Application to single photon detection, Nano Lett. **12,** 3501 (2012).

[19] M. Ejrnaes, D. Salvoni, L. Parlato, D. Massarotti, R. Caruso, F. Tafuri, X. Y. Yang, L. X. You, Z. Wang, G. P. Pepe, and R. Cristiano, Superconductor to resistive state switching by multiple fluctuation events in NbTiN nanostrips, Sci. Rep. **9,** 8053 (2019).

[20] K. Kato, T. Takagi, T. Tanabe, S. Moriyama, Y. Morita, and H. Maki, Manipulation of phase slips in carbon-nanotube-templated niobium-nitride superconducting nanowires under microwave radiation, Sci. Rep. **10,** 14278 (2020).

[21] M. Lyatti, M. A. Wolff, I. Gundareva, M. Kruth, S. Ferrari, R. E. Dunin-Borkowski, and C. Schuck, Energy-level quantization and single-photon control of phase slips in YBa$_2$Cu$_3$O$_{7-x}$ nanowires, Nat. Commun. **11,** 7639 (2020).

[22] M. Sahu, M. H. Bae, A. Rogachev, D. Pekker, T. C. Wei, N. Shah, P. M. Goldbart, and A. Bezryadin, Individual topological tunnelling events of a quantum field probed through their macroscopic consequences, Nat. Phys. **5**, 503 (2009).

[23] P. Li, P. M. Wu, Y. Bomze, I. V. Borzenets, G. Finkelstein, and A. M. Chang, Switching Currents Limited by Single Phase Slips in One-Dimensional Superconducting Al Nanowires, Phys. Rev. Lett. **107**, 137004 (2011).

[24] T. A. Fulton and L. N. Dunkleberger, Lifetime of zero-voltage state in josephson tunnel-junctions, Phys. Rev. B **9**, 4760 (1974).

[25] Q. Chen, B. Zhang, L. B. Zhang, R. Ge, R. Y. Xu, Y. Wu, X. C. Tu, X. Q. Jia, D. F. Pan, L. Kang, J. Chen, and P. H. Wu, Sixteen-pixel NbN nanowire single photon detector coupled with 300-$\mu$m fiber, IEEE Photonics J. **12**, 13 (2020).

[26] B. Zhang, Q. Chen, L. B. Zhang, R. Ge, J. R. Tan, X. Li, X. Q. Jia, L. Kang, and P. H. Wu, Approaching linear photon-number resolution with superconductor nanowire array, Appl. Phys. B: Lasers Opt. **126**, 59 (2020).

[27] W. A. Little, Decay of persistent currents in small superconductors, Phys. Rev. **156**, 396 (1967).

[28] A. D. Zaikin, D. S. Golubev, A. van Otterlo, and G. T. Zimanyi, Quantum Phase Slips and Transport in Ultrathin Superconducting Wires, Phys. Rev. Lett. **78**, 1552 (1997).

[29] D. S. Golubev and A. D. Zaikin, Quantum tunneling of the order parameter in superconducting nanowires, Phys. Rev. B **64**, 014504 (2001).

[30] J. Bardeen, Critical fields and currents in superconductors, Rev. Mod. Phys. **34**, 667 (1962).

[31] J. M. Martinis, M. H. Devoret, and J. Clarke, Experimental tests for the quantum behavior of a macroscopic degree of freedom: The phase difference across a josephson junction, Phys. Rev. B **35**, 4682 (1987).

[32] A. Engel, J. J. Renema, K. Il'in, and A. Semenov, Detection mechanism of superconducting nanowire single-photon detectors, Supercond. Sci. Technol. **28**, 114003 (2015).

[33] J. S. Langer and V. Ambegaokar, Intrinsic resistive transition in narrow superconducting channels, Phys. Rev. **164**, 498 (1967).

[34] A. Engel, J. Lonsky, X. F. Zhang, and A. Schilling, Detection mechanism in SNSPD: Numerical results of a conceptually simple, Yet powerful detection model, IEEE Trans. Appl. Supercond. **25**, 2200407 (2015).

[35] L. N. Bulaevskii, M. J. Graf, and V. G. Kogan, Vortex-assisted photon counts and their magnetic field dependence in single-photon superconducting detectors, Phys. Rev. B **85**, 014505 (2012).

[36] D. Y. Vodolazov, Current dependence of the red boundary of superconducting single-photon detectors in the modified hot-spot model, Phys. Rev. B **90**, 054515 (2014).

[37] A. N. Zotova and D. Y. Vodolazov, Intrinsic detection efficiency of superconducting nanowire single photon detector in the modified hot spot model, Supercond. Sci. Technol. **27**, 125001 (2014).

[38] J. Kitaygorsky, J. Zhang, A. Verevkin, A. Sergeev, A. Korneev, V. Matvienko, P. Kouminov, K. Smirnov, B. Voronov, G. Gol'tsman, and R. Sobolewski, Origin of dark counts in nanostructured NbN single-photon detectors, IEEE Trans. Appl. Supercond. **15**, 545 (2005).

[39] M. Bell, A. Sergeev, V. Mitin, J. Bird, A. Verevkin, and G. Gol'tsman, One-dimensional resistive states in quasi-two-dimensional superconductors: Experiment and theory, Phys. Rev. B **76**, 094521 (2007).